I&EC research
Industrial & Engineering Chemistry Research

Open Access
This article is licensed under CC-BY-NC-ND 4.0

pubs.acs.org/IECR
Article

Performance Assessment of a Membrane Gas Absorption (MGA) Process for Biogas Upgrading with Potassium-Based Solvents

Triantafyllia Grekou, Nikoleta Lazaridou, Maria V. Pagliaro, Hamish Andrew Miller, Ioannis Evgeniadis, Akrivi G. Asimakopoulou, Grigorios Pantoleontos, and Dimitrios Koutsonikolas*

Cite This: https://doi.org/10.1021/acs.iecr.6c02581

Read Online

ACCESS | Metrics & More | Article Recommendations

ABSTRACT: Global energy instability has increased interest in biomethane production through biogas upgrading as a renewable alternative to natural gas. This study experimentally investigated membrane gas absorption (MGA) for CO_2 capture using aqueous potassium hydroxide (KOH) and potassium carbonate (K_2CO_3) in a hydrophobic polypropylene hollow fiber membrane contactor under once-through and recycle operating modes. KOH demonstrated faster reaction kinetics and superior mass transfer performance, whereas K_2CO_3 exhibited slower but steadier CO_2 absorption behavior. Under recycle mode operation, both absorbents reached a comparable saturation capacity of approximately 1 mol of CO_2 per mol of absorbent despite their different absorption profiles. The membrane showed no measurable performance decline or morphological changes, confirming good membrane stability and compatibility with both solvents. The results demonstrate the potential of MGA as an effective and flexible approach for small- to medium-scale decentralized biogas upgrading using alkaline solvents with improved chemical stability, lower toxicity, and potential economic advantages over conventional amine-based absorbents.

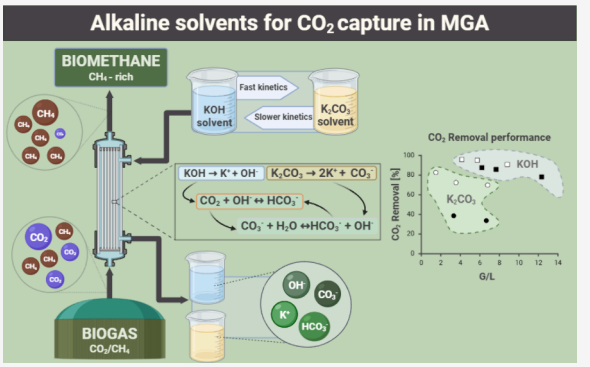

1. INTRODUCTION

The growing instability of global energy markets, coupled with ongoing geopolitical disruptions, has intensified the need for secure and domestically sourced energy systems, thereby enhancing the strategic role of biogas as a renewable energy carrier.[1] In this context, biomethane, derived from purified biogas, has attracted significant attention as a renewable alternative to natural gas.[2−5] The relevance of such alternatives is further underscored by recent trends, as global energy-related CO_2 emissions increased by 0.8% in 2024, reaching an all-time high of 37.8 Gt of CO_2, with emissions from natural gas rising by approximately 2.5% in 2024 (about 180 Mt of CO_2), representing the largest contribution to global carbon emissions growth.[6] Upgrading biogas to biomethane contributes to greenhouse gas (GHG) emissions mitigation by substituting fossil natural gas and supporting low-carbon energy systems.[7] Biogas is produced through anaerobic digestion of organic waste and typically contains 50%−75% methane (CH_4), 25%−50% CO_2, and trace gases such as hydrogen sulfide (H_2S).[8,9] The high CO_2 content reduces the calorific value, narrows flammability limits, decreases flame speed, and promotes corrosion of pipelines and equipment.[10,11] Therefore, efficient CO_2 removal is essential to improve biogas quality and enable its utilization as a substitute for natural gas.[12]

Building on the need for effective CO_2 removal, several separation technologies have been developed for biogas upgrading, among which membrane-based processes have emerged as a promising and increasingly commercialized option. Their modularity, compact design, and operational flexibility render them attractive for efficient and scalable biomethane production.[13,14] Membrane-based CO_2 separation technologies can be broadly classified into two main categories: (i) gas separation membranes, which rely on selective permeation, and (ii) membrane gas absorption (MGA) systems, where membrane contactors are combined with chemical absorption using a liquid solvent.[15] The latter approach integrates the advantages of conventional absorption with those of membrane technology, offering enhanced mass transfer performance and process intensification.[16] In MGA systems, a porous hydrophobic membrane acts as a non-dispersive interface between the gas and liquid phases, enabling a high specific interfacial area and independent control of gas

Received: May 19, 2026
Revised: July 20, 2026
Accepted: July 30, 2026

ACS Publications
© XXXX The Authors. Published by American Chemical Society

Downloaded from pubs.acs.org/iecred/article-pdf/doi/10.1021/acs.iecr.6c02581/6699023/acs.iecr.6c02581.pdf by guest on 26 August 2026

and liquid flow rates within a compact configuration. Consequently, common operational limitations of conventional absorption columns (e.g., flooding, foaming, and gas−liquid entrainment) are inherently avoided.[17−19] Moreover, MGA systems exhibit a fast dynamic response to fluctuations in operating conditions, ensuring high on-stream reliability and reducing downtime,[14,20,21] which is particularly advantageous in applications where energy efficiency and cost-effectiveness are critical. Additionally, MGA can be readily operated in stripping mode (reverse operation) after the absorption process, where a vacuum can be applied on the other side of the membrane contactor plus mild heating of the solvent in order to aid CO_2 desorption and solvent regeneration; note that the regeneration process can be facilitated more effectively in the physical absorption solvent case, with minimal energy requirements.[22−24] A summary of the advantages and limitations of each technology is presented in Table 1.

Table 1. Comparison between Packed Column and MGA Units for Gas Absorption−Regeneration Applications

Technology	Advantages	Limitations
Packed column absorption units	• Well-established technology • Flexible use of different solvents depending on the application	• Solvent foaming • Column flooding • Large equipment size • Solvent losses (particularly during solvent regeneration)
Membrane gas absorption units	• High gas−liquid interfacial area • Compact equipment size • No foaming or flooding • Simple and flexible operation • Modular and scalable design • Energy efficient regeneration	• Membrane pore wetting • Long-term membrane stability and durability • Solvent compatibility restrictions

Industrial applications of membrane contactors include water deionization, pharmaceutical and biotechnological processes, as well as applications in the beverage, oil, and gas industries, among others, as discussed by Sengupta and Peterson.[25]

The selection of the chemical solvent is a key factor governing CO_2 absorption performance in MGA systems. Conventional amine-based absorbents, such as monoethanolamine (MEA) and diethanolamine (DEA), are widely considered as benchmark solvents due to their fast reaction kinetics, high CO_2 removal efficiency, and successful industrial implementation in packed column absorption processes over several decades.[26−28] Amine solutions in MGA systems have been used in a number of cases;[29−32] see, for example, some remarks in the study by Pantoleontos et al.[5] especially regarding the use of MEA solutions in MGA systems and their limitations.

However, despite their excellent absorption characteristics, amine-based solutions suffer from several limitations, including equipment corrosion, solvent degradation and oxidation in the presence of O_2, NO_x, and SO_x, toxicity concerns, susceptibility to membrane wetting, and high regeneration energy demand due to the elevated temperatures required for solvent recovery.[33−37] To address these challenges, increasing attention has been directed toward alternative solvents for CO_2 capture, such as potassium-based alkaline absorbents like potassium hydroxide (KOH) and potassium carbonate (K_2CO_3).[38−43] Compared to amine-based solutions, these solvents exhibit improved chemical stability and compatibility with the membranes, lower regeneration energy demands, lower cost, and reduced environmental impact.[40] Among them, potassium carbonate is especially attractive due to its high CO_2 loading capacity, low regeneration energy requirements, reduced toxicity and corrosivity, and enhanced thermal stability, although it is generally characterized by slower reaction kinetics compared to potassium hydroxide.[41,43−45] Furthermore, it should be noted that absorption of CO_2 into K_2CO_3 leads to the formation of less soluble $KHCO_3$. While aqueous solutions containing more than 40% w/w K_2CO_3 may promote potassium bicarbonate crystallization, the stable operation of membrane contactors can be achieved by maintaining operating conditions below the precipitation values, thereby preventing membrane fouling, pore blockage, and increased mass transfer resistance.[46,47] Moreover, these solvents are increasingly being considered in advanced CCUS schemes involving either electrochemical regeneration of the solvent[48] or the direct electrochemical conversion of captured CO_2 to potassium formate,[49,50] thereby offering opportunities for flexible, electricity-driven operation under conditions of surplus renewable power.

In this study, the performance of an MGA process for CO_2 capture and biogas upgrading is evaluated using hydrophobic polypropylene (PP) hollow fiber membranes as the gas−liquid contactor and aqueous KOH and K_2CO_3 solvents at a concentration of 1.0 M. Experiments are conducted under both once-through and solvent recycle modes to systematically assess absorption performance and operational behavior under conditions relevant to biogas upgrading. Although alkaline solvents have been extensively investigated for CO_2 capture in conventional absorption processes, their application in MGA configurations, particularly under biogas-relevant conditions, remains relatively underexplored. Therefore, this study aims to define the performance envelope of KOH- and K_2CO_3-based MGA systems and elucidate their potential for efficient and scalable CO_2 removal in biogas upgrading applications.

2. EXPERIMENTAL SECTION

2.1. Experimental Setup

The piping and instrumentation diagram of the MGA unit is illustrated in Figure 1. The experimental setup is designed to enable controlled gas−liquid contact within a hollow fiber membrane module operating in a counter-current flow configuration. Figure 2 illustrates a typical configuration of the contactor. The gas phase is typically introduced through the lumen side (inner channel) of the fibers, while the liquid absorbent flows through the shell side (outer channel).

The gas is delivered from gas cylinders through pressure regulators to the mass flow controllers (EL-Flow Select, Bronkhorst), which accurately adjust and maintain the desired inlet gas flow rates. The volumetric gas flow rates at the inlet and outlet of the membrane module may be continuously measured using a drum-type flowmeter (Ritter TG1/5), while gas composition is monitored using an online infrared biogas analyzer (Hubei Cubic-Ruiyi, Gasboard-3200), with measurement ranges of CH_4, 0−100%; CO_2, 0−50%; H_2S, 0−9999 ppm; and O_2, 0−25%. The liquid solvent is supplied from an external tank (maximum capacity: 4 L) and delivered to the system using a peristaltic pump (Ismatec BVP-Z). A set of dedicated tubes and valves allows flexible operation, enabling the gas and liquid streams to be directed either through the membrane contactor or to bypass it,

Downloaded from pubs.acs.org/iecred/article-pdf/doi/10.1021/acs.iecr.6c02581/6699023/acs.iecr.6c02581.pdf by guest on 26 August 2026

https://doi.org/10.1021/acs.iecr.6c02581
Ind. Eng. Chem. Res. XXXX, XXX, XXX−XXX

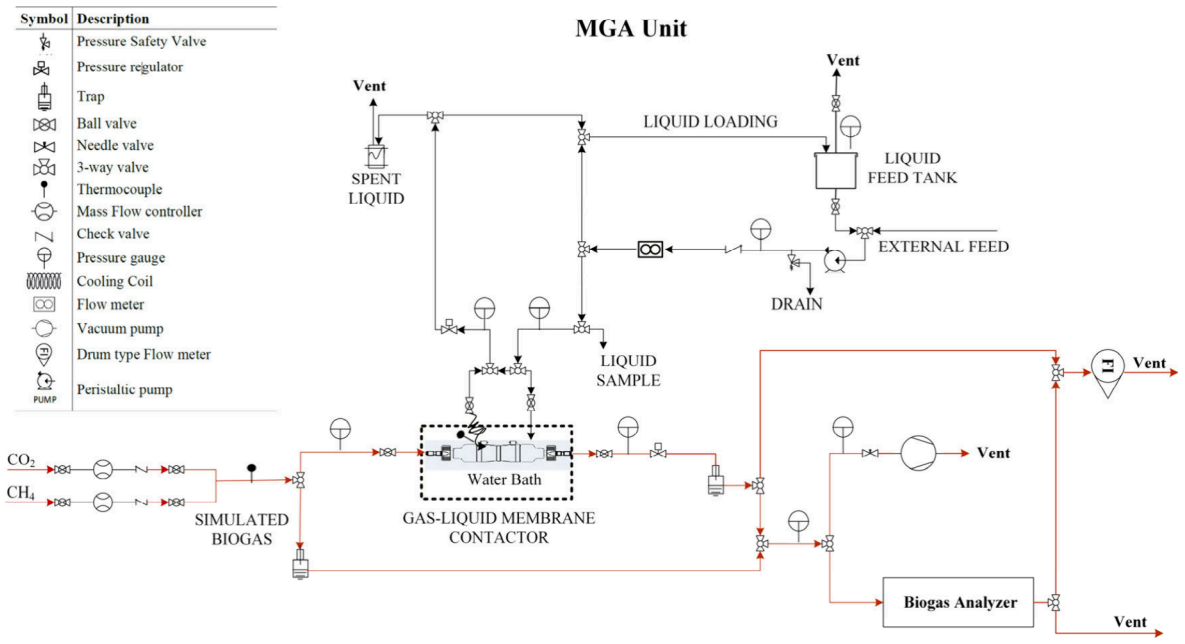

Figure 1. Piping and instrumentationdiagram of the membrane gas absorption (MGA) unit for carbon capture.

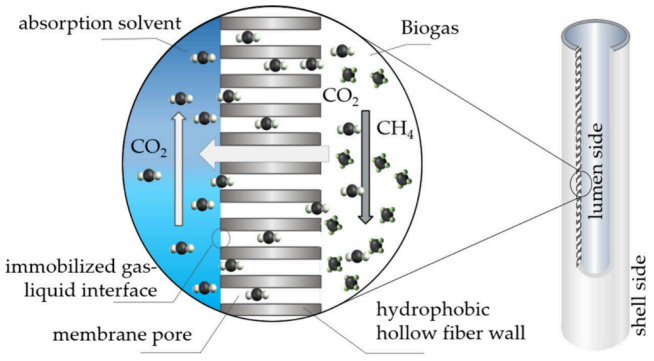

Figure 2. Schematic representation of the membrane gas absorption (MGA) process. The figure shows the gas–liquid interface within the pores of hydrophobic hollow fibers, enabling selective chemical absorption.[39]

depending on the required experimental configuration. Temperature, pressure, and flow rates are continuously monitored throughout all experiments. This configuration enables the systematic investigation of both steady-state and dynamic operating conditions relevant to biogas upgrading. Specifically, under the once-through operation, the solvent exiting the module is collected in a downstream container, while in the recycle mode, the solvent is continuously returned to the feed reservoir, allowing the evaluation of the absorption performance under progressively increasing CO_2 loading.

2.2. CO_2 Capture Experiments

A commercial 3M Liqui-Cel hollow fiber membrane contactor, model MM-1.7X5.5, was employed as the gas–liquid contacting unit. The module comprises approximately 7400 X50 porous hydrophobic polypropylene hollow fibers, each with an outer diameter (OD) of 300 μm and an inner diameter (ID) of 220 μm, providing an effective membrane surface area (OD-based) of approximately 0.79 m^2.

Each experimental run commenced with the preparation of fresh solvent solutions by dissolving potassium hydroxide (KOH) pellets (≥85% purity; Chem-Lab) and potassium carbonate (K_2CO_3) powder (≥98% purity; Chem-Lab) in deionized water to obtain 1 M aqueous solutions. The solvents were introduced into the system with the dedicated pump at pressures 0.2–0.3 barg, slightly higher than the gas-phase pressure, ensuring complete filling of the shell side while avoiding undesired phase dispersion and minimizing long-term membrane wetting effects.

Prior to each experiment, the gas analyzers were warmed up and calibrated using standard gas mixtures representative of the operating conditions. The gas phase consisted of premixed simulated biogas of 45% CO_2 in CH_4, supplied from a gas cylinder (Air Products and Chemicals, Inc.). The feed gas composition and flow rate were set and verified before the gas entered the membrane module, with initial stabilization performed via a bypass line. Following stabilization, the gas stream was directed into the lumen side of the membrane module under counter-current flow conditions. For each set of operating parameters, the outlet gas composition and flow rate were continuously monitored until either (i) steady-state conditions were achieved in once-through operation mode (typically within ~10 min) or (ii) the gas outlet concentration of CO_2 approached that of the gas inlet in recycle operation mode.

2.3. Membrane Compatibility Assessment Tests

Membrane compatibility with the alkaline solvents was evaluated through dedicated exposure experiments using two 3M Liqui-Cel MM-0.5X1 series membrane contactors with an effective membrane area of 0.01 m^2 operating in a continuous solvent recycle mode for a total of 4 days. One module was tested with 1 M KOH, and the other was tested with 1 M K_2CO_3. During the first 2 days, each system was operated under an inert nitrogen atmosphere (100% N_2), while during the subsequent 2 days the gas feed was switched to simulated biogas composition containing 45% CO_2, allowing the membranes to be exposed to both fresh and CO_2 loaded absorbents. Throughout these experimental tests, gas and liquid flow rates were maintained at 0.16 L/min and 0.1 L/min, respectively. After completion of the exposure tests, membrane samples were extracted and analyzed using scanning electron microscopy to assess potential changes in the membrane surface morphology and structural integrity. A pristine, unexposed membrane contactor of the same series was used as a reference comparison. Scanning electron microscopy (SEM) sample characterization was performed using a TESCAN Gaia 3 FIB/SEM instrument. The microscope hosts a 30 kV Triglav electron column and a Cobra Focused Gallium Ion Beam column. SEM images of the sample surfaces were acquired using the two in-beam secondary electron (SE) and backscattered electron (BSE) detectors located inside the electron column. Samples were sputter-coated with a conductive metal and mounted on stubs. SEM images of the tubular

Downloaded from pubs.acs.org/iecred/article-pdf/doi/10.1021/acs.iecr.6c02581/6699023/acs.iecr.6c02581.pdf by guest on 26 August 2026

https://doi.org/10.1021/acs.iecr.6c02581
Ind. Eng. Chem. Res. XXXX, XXX, XXX–XXX

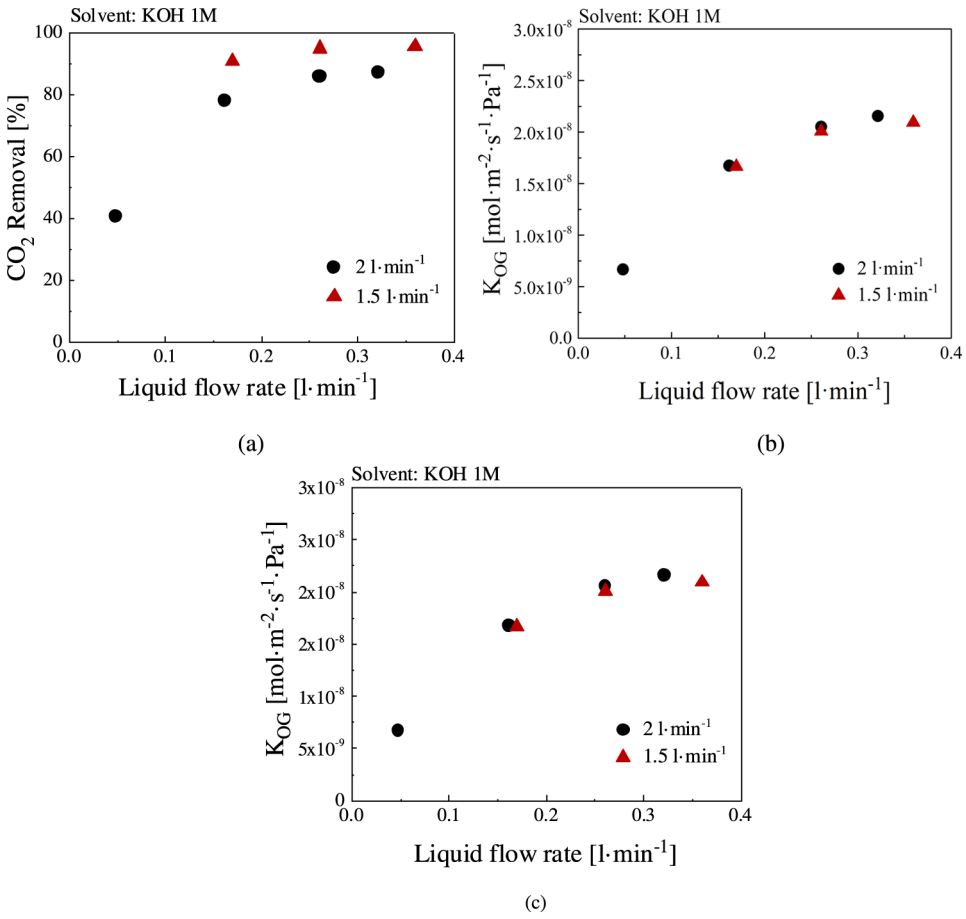

Figure 3. Effect of gas and liquid flow rate on CO_2 removal (a), CO_2 absorption flux (b), and overall mass transfer coefficient (c) for solvent 1 M KOH at different inlet gas flow rates (1.5 and 2 L/min).

structures were acquired at 5 kV using the in-beam SE detector, highlighting the surface morphology in detail.

2.4. Analysis of Experimental Measurements

CO_2 removal using aqueous solutions of KOH and K_2CO_3 proceeds via chemical absorption, where CO_2 reacts with the alkaline species to form bicarbonate ions. While the current study is focused on the experimental procedures and performance assessment, the reactions of carbonate solutions merit discussion, as they provide insights into the CO_2 removal efficiency of KOH and K_2CO_3 systems. The overall mechanism is governed by a set of coupled reactions. The primary absorption reaction involves the formation of bicarbonate from dissolved CO_2 and hydroxide ions:

$$CO_2 + OH^- \leftrightarrow HCO_3^- \quad \text{(AR1)}$$

In addition, the carbonate–bicarbonate equilibrium contributes to the generation of hydroxide ions:

$$CO_3^{2-} + H_2O \leftrightarrow HCO_3^- + OH^- \quad \text{(AR2)}$$

Reaction AR2 is typically assumed to be at equilibrium. The availability of reactive species depends on the dissociation of the respective potassium-based solvents:

$$KOH \rightarrow K^+ + OH^- \quad \text{(AR3)}$$

$$K_2CO_3 \rightarrow 2K^+ + CO_3^{2-} \quad \text{(AR4)}$$

Complete dissociation is generally assumed for both of the salts. In KOH solutions, hydroxide ions are directly available for the reaction with CO_2 via reaction AR1. In contrast, in K_2CO_3 systems, hydroxide ions are generated indirectly through the carbonate equilibrium (reaction AR2), making the carbonate concentration a key parameter governing hydroxide availability. In both cases, bicarbonate (HCO_3^-) is the dominant reaction product, formed through the combined contribution of the kinetic absorption reaction (reaction AR1) and the equilibrium reaction (reaction AR2).[51]

Experimental data, combined with mass balance relationships, were used to determine the key performance indicators of the process, including the CO_2 removal efficiency, solvent loading, CO_2 absorption flux, and overall apparent mass transfer coefficient.

The CO_2 removal efficiency (eq 1) is calculated as

$$CO_2 \text{ removal } (\%) = \frac{Q_{CO2,in} - Q_{CO2,out}}{Q_{CO2,in}} \times 100 \quad (1)$$

where $Q_{CO2,in}$ and $Q_{CO2,out}$ are the molar flow rates (mol/s) of CO_2 at the inlet and outlet of the membrane module, respectively. The volumetric gas flow rate was converted to molar flow rate using the ideal gas law, accounting for the operating temperature and pressure.

The solvent loading, a (mol of CO_2 per mol of absorbent), is defined as

$$a = \frac{mol_{CO2,L}}{mol_{absorbent}} = \frac{Q_{CO2,in} - Q_{CO2,out}}{C_{absorbent} \times F_{solvent}} \quad (2)$$

where $mol_{CO2,L}$ is the moles of CO_2 absorbed in the solvent (mol), $mol_{absorbent}$ is the moles of the absorbent in the solvent (mol), $C_{absorbent}$ (mol/L) is the concentration of the absorbent in the solvent, and $F_{solvent}$ (L/s) is the volumetric flow rate of the solvent, which is an experimental parameter.

The overall molar flux of CO_2, J_{CO2} (mol s^{-1} m^{-2}), through the membrane into the shell side is given by

Downloaded from pubs.acs.org/iecred/article-pdf/doi/10.1021/acs.iecr.6c02581/6699023/acs.iecr.6c02581.pdf by guest on 26 August 2026

https://doi.org/10.1021/acs.iecr.6c02581
Ind. Eng. Chem. Res. XXXX, XXX, XXX−XXX

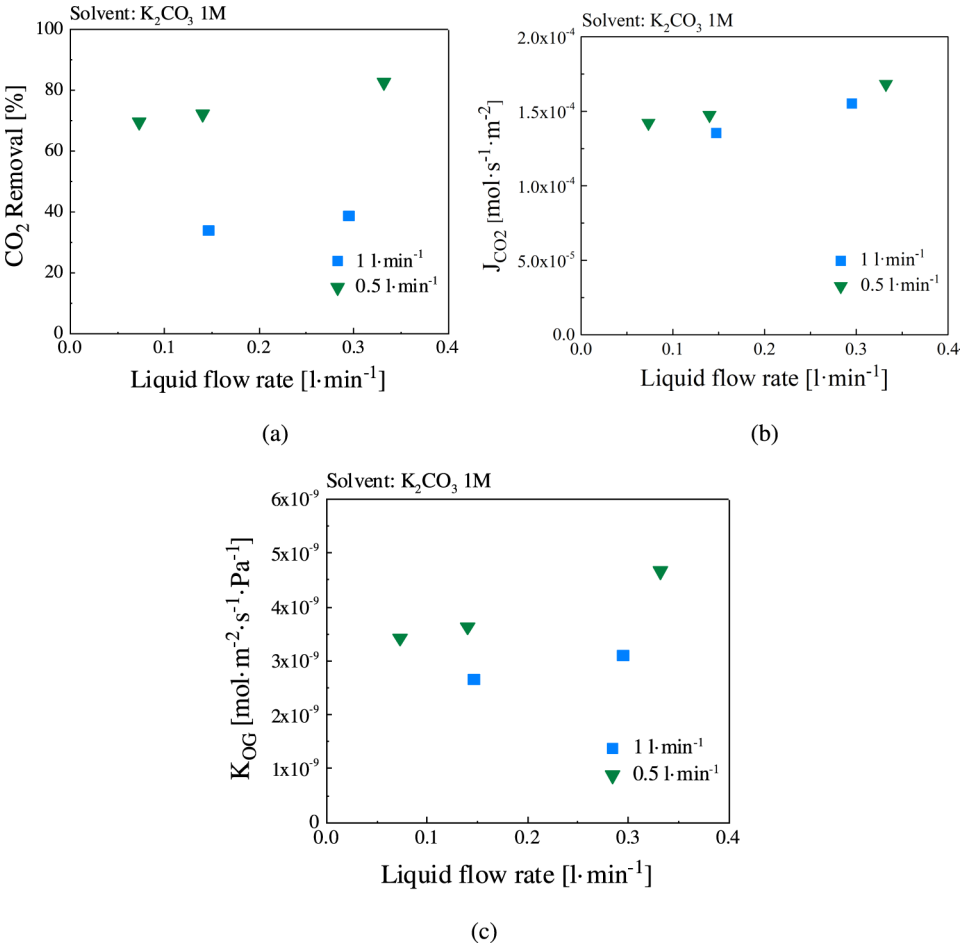

Figure 4. Effect of gas and liquid flow rate on CO_2 removal (a), CO_2 absorption flux (b), and overall mass transfer coefficient (c) for solvent 1 M K_2CO_3 at different inlet gas flow rates (0.5 and 1 L/min).

$$J_{CO2} = \frac{Q_{CO2,in} - Q_{CO2,out}}{A} \quad (3)$$

where A (m^2) is the effective membrane surface area.

The overall apparent mass transfer coefficient, K_{OG} (mol m^{-2} s^{-1} Pa^{-1}), is calculated as

$$K_{OG} = \frac{J_{CO2}}{\Delta P_{CO2,lm}} \quad (4)$$

where $\Delta P_{CO2,lm}$ (Pa) is the logarithmic mean CO_2 partial pressure difference between the gas and liquid phase:

$$\Delta P_{CO2,lm} = \frac{(P_{CO2,in} - P_{CO2,L,out}^*) - (P_{CO2,out} - P_{CO2,L,in}^*)}{\ln\left(\frac{P_{CO2,in} - P_{CO2,L,out}^*}{P_{CO2,out} - P_{CO2,L,in}^*}\right)} \quad (5)$$

where$P_{CO2,in}$ and $P_{CO2,out}$ (Pa) are the CO_2 partial pressures in the gas phase entering and exiting the module, respectively, which are experimentally recorded, while $P_{CO2,L,in}$* and $P_{CO2,L,out}$* (Pa) are the partial equilibrium pressures of CO_2 at the liquid inlet and outlet streams, respectively.

Due to the fast reaction between CO_2 and alkaline solvents, the concentration of physically dissolved CO_2 in the liquid phase is typically negligible. Under this assumption, the mass transfer driving force can be expressed using the logarithmic mean partial pressure difference based on the corresponding CO_2 mole fractions (LMPD). Consequently, eq 5 may be accordingly simplified to eq 6:[52]

$$\Delta P_{CO2,lm} = \text{LMPD} = P_{inert}\frac{Y_{in} - Y_{out}}{\ln\left(\frac{Y_{in}}{Y_{out}}\right)} \quad (6)$$

where Y_{in} and Y_{out} $\left(\frac{mol_{CO2}}{mol_{inert}}\right)$ are the mole ratios of CO_2 to inert gas in the gas phase, while P_{inert} (Pa) is the partial pressure of the inert gas.

3. RESULTS AND DISCUSSION

3.1. Solvent Once-Through Absorption Tests

The CO_2 absorption performance of aqueous KOH and K_2CO_3 solutions was experimentally evaluated through both solvent once-through and recycle mode tests. Initially, key performance indicators, including the CO_2 removal efficiency, CO_2 absorption flux, and overall apparent mass transfer coefficient (K_{OG}), were determined as a function of the gas and liquid flow rates. Subsequently, each solvent's saturation behavior was investigated under the solvent recycle operation mode.

Figures 3 and 4 present the experimental results as a function of the liquid flow rate, for two different gas flow rates, using 1 M KOH and 1 M K_2CO_3, respectively. In all cases, a simulated biogas stream (45% CO_2 in CH_4) was used as feed gas. The operating conditions were selected to capture the observed trends over a practically relevant range of CO_2 removal efficiencies. Furthermore, for the KOH system operating at a gas flow rate of 2 L/min, an additional point

https://doi.org/10.1021/acs.iecr.6c02581
Ind. Eng. Chem. Res. XXXX, XXX, XXX−XXX

Downloaded from pubs.acs.org/iecred/article-pdf/doi/10.1021/acs.iecr.6c02581/6699023/acs.iecr.6c02581.pdf by guest on 26 August 2026

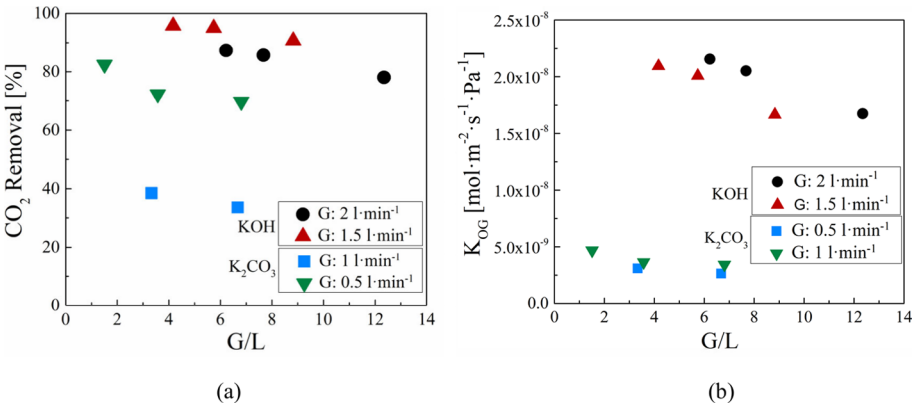

Figure 5. Comparison of the overall CO_2 removal efficiency (%) (a) and mass transfer coefficients (b) using 1 M KOH and 1 M K_2CO_3 solutions in a polypropylene (PP) hollow fiber membrane contactor for different gas-to-liquid flow rate ratios (G/L) at different inlet gas flow rates (0.5−2 L/min).

was included to extend the analysis toward lower CO_2 removal efficiencies. Nevertheless, in all experiments, a minimum CO_2 removal efficiency of 30% was ensured. Notably, substantially lower gas flow rates were required for the 1 M K_2CO_3 absorbent compared to 1 M KOH in order to achieve the same removal efficiencies, owing to the slower reaction kinetics of the former.

For both solvents, increasing the liquid flow rate resulted in higher CO_2 removal efficiencies, increased CO_2 absorption fluxes, and enhanced overall mass transfer coefficients. This behavior is attributed to improved local liquid-side mass transfer, driven by higher liquid velocities, and reduced solvent saturation, as the reactive species in the solvent are ubiquitous, thus promoting CO_2 absorption.[52,53] For KOH, the CO_2 flux exhibited a steep increase as the liquid flow rate increased from 0.05 to 0.16 L/min, beyond which a plateau was observed, indicating that beyond this point the available reactive species are in excess and the liquid-phase mass transfer resistance is negligible compared to the combined membrane and gas-phase resistance. A similar behavior has been observed for fast-reacting solvents, such as monoethanolamine (MEA).[53] In contrast to KOH, no clear plateau was observed for K_2CO_3 under the investigated conditions, suggesting that in the whole range of the liquid flow rate tested, the liquid-phase mass transfer resistance remains comparable to the combined membrane and gas-phase resistance, due to the slower absorption kinetics.

The effect of the gas flow rate on the CO_2 absorption efficiency is also evident in Figures 3 and 4. Increasing the gas flow rate led to a decrease in the CO_2 removal efficiency, primarily due to the reduced gas residence time and the shorter gas−liquid contact. This behavior is in good agreement with previously reported studies.[53,54] For the KOH system, higher gas flow rates resulted in increased CO_2 flux (Figure 3b) due to enhanced gas−liquid mass transfer driven by increased gas velocities (i.e., increased local mass transfer coefficients) and driving forces (due to lower removal efficiencies).[53] This trend was not observed for K_2CO_3 (Figure 4b), further confirming that the rate-limiting step in carbonate-based systems is governed by the slower reaction kinetics at the gas−liquid interface rather than by gas-phase mass transfer limitations. This interpretation is further supported by the substantially lower mass transfer coefficients calculated for K_2CO_3 (Figure 5b), confirming that slower liquid-side reaction kinetics constitute the controlling step for the carbonate-based solvent.

Figure 5 presents an attempt to summarize the CO_2 removal efficiency and the apparent overall mass transfer coefficient per solvent, as a function of the gas-to-liquid (G/L) flow rate ratio. This approach was not successful for the CO_2 removal efficiency, as this metric reflects overall process performance and is independently affected by multiple operating parameters, including the gas flow rate, liquid flow rate, and available membrane area. Consequently, the results could not be consistently grouped by solvent using the G/L ratio as the sole variable. As shown in Figure 5a, the CO_2 removal efficiency varied substantially at the same G/L ratio, even for the same solvent, when different gas flow rates were applied. The figure also shows that, with 1 M K_2CO_3, CO_2 removal efficiencies above 70% were achieved at considerably lower gas flow rates than those used with 1 M KOH. In contrast, the grouping approach proved more suitable for the apparent overall mass transfer coefficient (K_{OG}), which is a more fundamental parameter reflecting the combined effects of mass transfer and reaction kinetics and therefore allows a more direct comparison between solvents. As illustrated in Figure 5b, K_{OG} values obtained at different gas flow rates could be grouped reasonably well by solvent using the G/L ratio alone. Moreover, regardless of the CO_2 removal efficiency achieved, KOH consistently exhibited substantially higher K_{OG} values (16.7×10^{-9}−20.9×10^{-9} mol m^{-2} s^{-1} Pa^{-1}) than K_2CO_3 (2.6×10^{-9}−4.7×10^{-9} mol m^{-2} s^{-1} Pa^{-1}) across all G/L ratios, confirming the faster reaction kinetics of KOH with CO_2. For both solvents, K_{OG} decreased with increasing G/L ratio (with a steeper decline observed for KOH), indicating a higher overall mass transfer resistance (inverse K_{OG}) at increased G/L flow conditions.

3.2. Solvent Recycle Mode Absorption Tests

Two recycle mode experiments, one with 1 M KOH and one with 1 M K_2CO_3, were conducted to assess the solvent loading behavior and long-term CO_2 absorption performance. In each recycle experiment, the simulated biogas stream was continuously fed to the lumen side, while the solvent was continuously recirculated on the shell side. Specifically, the solvent exiting the membrane contactor was returned to the feed tank and recirculated back to the membrane, in contrast to the once-through experiments, where the solvent was discharged after a single pass and collected as waste. The outlet CO_2 concentration was monitored over time to assess the absorption performance (Figure 6), with gas flow rates set to 1

Downloaded from pubs.acs.org/iecred/article-pdf/doi/10.1021/acs.iecr.6c02581/6699023/acs.iecr.6c02581.pdf by guest on 26 August 2026

https://doi.org/10.1021/acs.iecr.6c02581
Ind. Eng. Chem. Res. XXXX, XXX, XXX−XXX

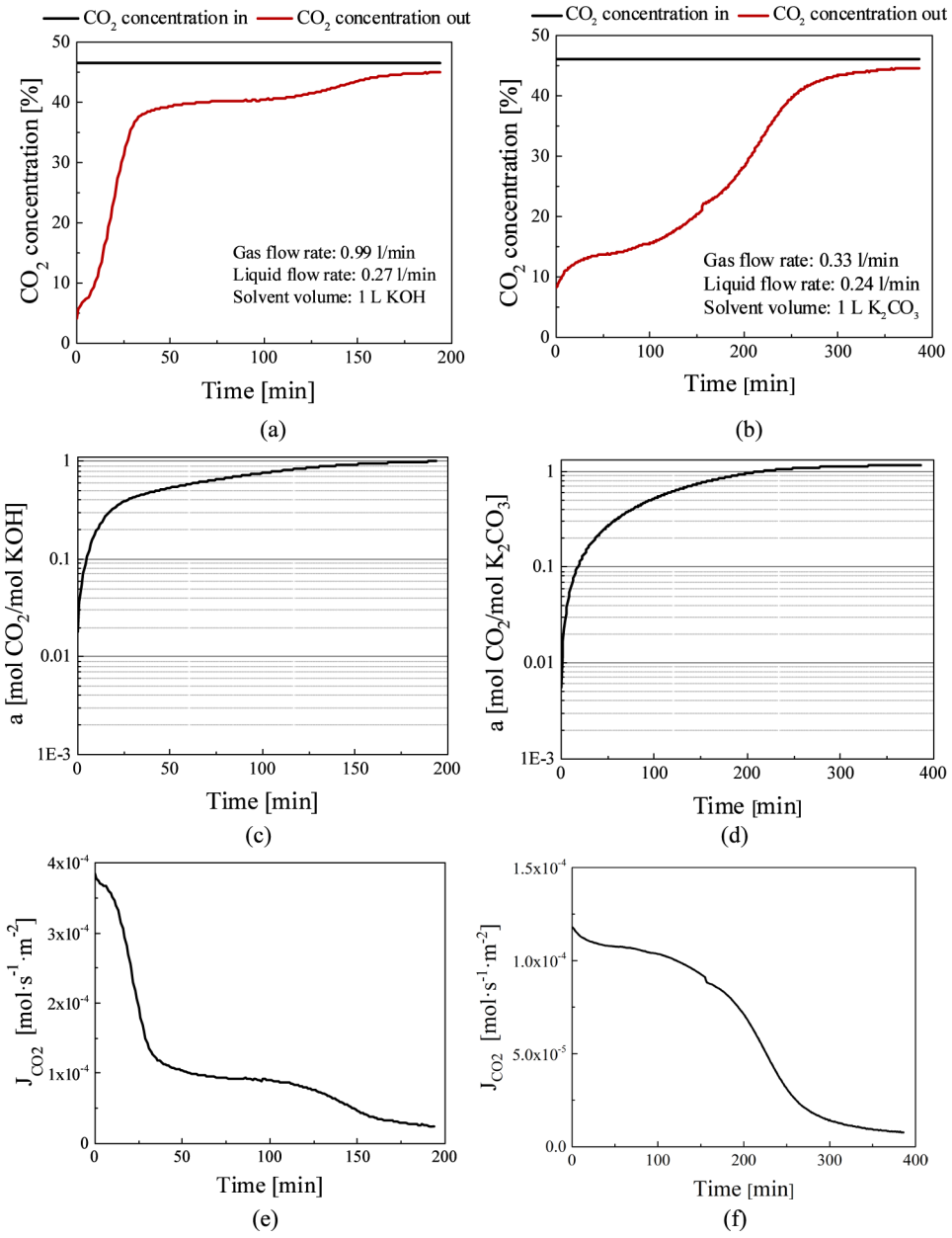

Figure 6. Solvent recycle mode performance during CO_2 absorption using 1 M KOH (a,c,e) and 1 M K_2CO_3 (b,d,f). Inlet and outlet CO_2 concentrations (a,b), solvent loading (c,d) , and CO^2 absorption flux(e,f).

L/min for KOH and 0.33 L/min for K_2CO_3, to ensure comparable initial conditions, i.e., an initial outlet CO_2 concentration below 10%, which facilitated data interpretation and minimized measurement uncertainty.

Figure 6a,b shows the measured outlet CO_2 concentration as a function of time, while Figure 6c,d presents the corresponding solvent loading profiles. The 1 M KOH solution exhibited a rapid initial CO_2 uptake due to the fast reaction with CO_2 to form bicarbonates. As KOH was consumed, the reaction rate declined, and the system gradually entered a slower regime. Consequently, the loading curve asymptotically approached a plateau near 1 mol of CO_2 per mol of KOH. In contrast, 1 M K_2CO_3 exhibited a slower but steady increase in the CO_2 loading, consistent with its slower intrinsic reaction kinetics associated with the carbonate-to-bicarbonate pathway. Nevertheless, the loading curve also approached asymptotically similar saturation levels, around 1 mol of CO_2 per mol of K_2CO_3.

The corresponding CO_2 flux profiles (Figure 6e,f for 1 M KOH and 1 M K_2CO_3, respectively) further illustrate these differences. In all cases, the CO_2 absorption flux decreased as the CO_2 loading of the solvent increased, in agreement with trends reported in the literature.[52,53,55] For the KOH system, the CO_2 flux was initially high, indicating strong absorption driven by the rapid reaction with KOH, but it decreased rapidly as the KOH was progressively consumed. After this point, the flux stabilized at a lower level until a new slow decline was observed as the solvent approached saturation. For the K_2CO_3 system, the initial CO_2 flux was moderately high due to the favorable concentration gradient and the availability of fresh absorbent. As absorption progressed and the solvent became increasingly loaded, the flux gradually decreased, reflecting the diminishing driving force and the reduced

Downloaded from pubs.acs.org/iecred/article-pdf/doi/10.1021/acs.iecr.6c02581/6699023/acs.iecr.6c02581.pdf by guest on 26 August 2026

https://doi.org/10.1021/acs.iecr.6c02581
Ind. Eng. Chem. Res. XXXX, XXX, XXX−XXX

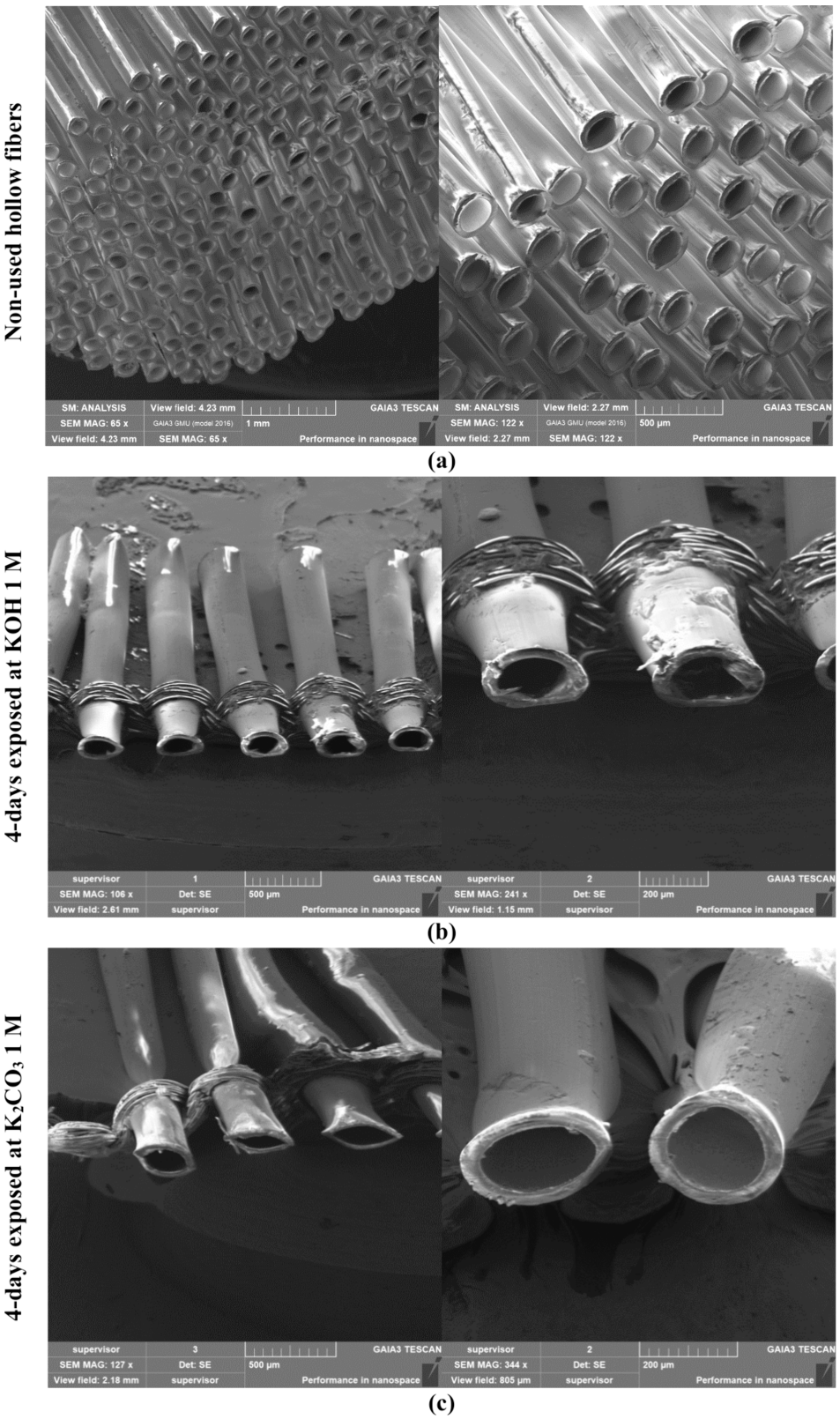

Figure 7. SEM images of the membrane contactor's hollow fibers before (a) and after 4 days of exposure to aqueous solvents of 1 M KOH (b) and 1 M K_2CO_3 (c) at different magnifications.

availability of reactive carbonate ions. Eventually, the flux stabilized at a low level and finally declined as the solvent approached full saturation, indicating the exhaustion of its CO_2 absorption capacity.

Overall, the combined once-through and recycle mode results demonstrate the superior performance of KOH in MGA, which is attributed to its rapid reaction kinetics with CO_2. Under identical operating conditions (gas and liquid flow rates), the CO_2 removal achieved with 1 M KOH was found to

https://doi.org/10.1021/acs.iecr.6c02581
Ind. Eng. Chem. Res. XXXX, XXX, XXX−XXX

Downloaded from pubs.acs.org/iecred/article-pdf/doi/10.1021/acs.iecr.6c02581/6899234/acs.iecr.6c02581.pdf by guest on 26 August 2026

be comparable to, and in some cases slightly higher than, that previously reported for a 0.25 M DEA solution in the same MGA configuration by our group,[5] indicating that KOH can provide competitive separation performance while offering additional advantages, such as lower solvent cost, higher chemical stability, reduced solvent degradation, and lower regeneration energy requirements. In contrast, K_2CO_3 exhibited a slower absorption performance, resulting in lower CO_2 removal under identical conditions. This kinetic limitation could be effectively addressed through the use of promoters[40,44] or blended KOH/K_2CO_3 mixtures,[42] which have been studied and shown to substantially enhance CO_2 absorption kinetics while retaining the favorable characteristics of K_2CO_3. Despite their different absorption rates, both alkaline solvents exhibited similar saturation capacities, approaching approximately 1 mol of CO_2 per mol of KOH or K_2CO_3, highlighting the long-term potential of potassium-based absorbents for membrane gas absorption applications.

3.3. Membrane Compatibility Investigation

Throughout the experimental test campaign, no significant performance loss was observed over time for the single membrane module (3M Liqui-Cel MM-1.7X5.5), indicating good membrane compatibility with the selected solvents. This observation was further supported by dedicated membrane exposure tests aiming to qualitatively assess the effects of chemical exposure and gas−liquid interactions on membrane structural integrity and surface morphology. Following the 4 day exposure period described in Section 2.3, three hollow fiber samples, one from the pristine membrane contactor and two from the membrane contactors exposed to 1 M KOH and 1 M K_2CO_3, respectively, were analyzed via scanning electron microscopy (SEM). The obtained SEM images are presented in Figure 7. No noticeable changes in the membrane's surface morphology were observed after exposure to either solvent. In addition, no potassium bicarbonate crystallization particles were detected on the membrane surface, implying that pore blockage or significant membrane degradation did not occur during the 4 day exposure period.

4. CONCLUSIONS

The present study experimentally evaluated membrane gas absorption (MGA) for CO_2 capture from simulated biogas streams by using aqueous KOH and K_2CO_3 solutions. The performance of both absorbents was investigated through once-through and recycle mode operation tests using a hydrophobic polypropylene hollow fiber membrane contactor.

In the once-through operation, both solvents showed improved CO_2 removal efficiency, CO_2 flux, and apparent overall mass transfer coefficient (K_{OG}) with increasing liquid flow rate, confirming the importance of enhanced liquid-side hydrodynamics and reduced solvent saturation (excess reactive species). KOH generally exhibited a higher mass transfer performance than K_2CO_3, with substantially higher K_{OG} values across all investigated gas-to-liquid ratios, reflecting its faster reaction kinetics with CO_2. For KOH, the CO_2 flux reached a plateau at higher liquid flow rates, indicating that liquid-phase resistance became negligible relative to the membrane and gas-phase resistances. By contrast, no such plateau was observed for K_2CO_3, suggesting that the liquid-phase resistance remained significant throughout the investigated range due to the slower reaction kinetics.

In the recycle mode operation, the two solvents exhibited distinct loading and flux evolution profiles, but both approached a similar saturation capacity of approximately 1 mol of CO_2 per mol of solvent. KOH showed rapid initial CO_2 uptake and high initial flux, followed by a marked decline as the active hydroxide was consumed, whereas K_2CO_3 displayed a slower but more gradual and stable absorption behavior consistent with the carbonate-to-bicarbonate reaction pathway. These findings indicate that KOH is better suited to applications requiring high absorption rates and superior mass transfer performance, while K_2CO_3 may remain attractive where slower but steadier absorption, together with a more favorable health, toxicity, and corrosivity profile, is desirable.

Finally, the absence of measurable membrane performance loss and morphological changes after solvent exposure indicate good membrane stability and compatibility with both absorbents.

AUTHOR INFORMATION

Corresponding Author

Dimitrios Koutsonikolas − *Laboratory of Advanced Renewable Technologies & Environmental Materials in Integrated Systems (ARTEMIS), Chemical Process & Energy Resources Institute (CPERI), Centre for Research & Technology Hellas (CERTH), 57001 Thermi-Thessaloniki, Greece;* orcid.org/0000-0002-2466-5619; Email: dkoutson@certh.gr

Authors

Triantafyllia Grekou − *Laboratory of Advanced Renewable Technologies & Environmental Materials in Integrated Systems (ARTEMIS), Chemical Process & Energy Resources Institute (CPERI), Centre for Research & Technology Hellas (CERTH), 57001 Thermi-Thessaloniki, Greece*

Nikoleta Lazaridou − *Laboratory of Advanced Renewable Technologies & Environmental Materials in Integrated Systems (ARTEMIS), Chemical Process & Energy Resources Institute (CPERI), Centre for Research & Technology Hellas (CERTH), 57001 Thermi-Thessaloniki, Greece*

Maria V. Pagliaro − *Institute of Chemistry of Organometallic Compounds (ICCOM), National Research Council of Italy (CNR), 50019 Sesto Fiorentino, Italy;* orcid.org/0000-0002-8385-6255

Hamish Andrew Miller − *Institute of Chemistry of Organometallic Compounds (ICCOM), National Research Council of Italy (CNR), 50019 Sesto Fiorentino, Italy;* orcid.org/0000-0003-1668-6476

Ioannis Evgeniadis − *Laboratory of Advanced Renewable Technologies & Environmental Materials in Integrated Systems (ARTEMIS), Chemical Process & Energy Resources Institute (CPERI), Centre for Research & Technology Hellas (CERTH), 57001 Thermi-Thessaloniki, Greece;* orcid.org/0009-0003-1993-2430

Akrivi G. Asimakopoulou − *Laboratory of Advanced Renewable Technologies & Environmental Materials in Integrated Systems (ARTEMIS), Chemical Process & Energy Resources Institute (CPERI), Centre for Research & Technology Hellas (CERTH), 57001 Thermi-Thessaloniki, Greece*

Grigorios Pantoleontos − *Laboratory of Advanced Renewable Technologies & Environmental Materials in Integrated Systems (ARTEMIS), Chemical Process & Energy Resources Institute (CPERI), Centre for Research & Technology Hellas*

Downloaded from pubs.acs.org/iecred/article-pdf/doi/10.1021/acs.iecr.6c02581/6699023/acs.iecr.6c02581.pdf by guest on 26 August 2026

https://doi.org/10.1021/acs.iecr.6c02581
Ind. Eng. Chem. Res. XXXX, XXX, XXX−XXX

(CERTH), 57001 Thermi-Thessaloniki, Greece;
orcid.org/0000-0001-8166-1588

Complete contact information is available at:
https://pubs.acs.org/10.1021/acs.iecr.6c02581

Funding

The open access publishing of this article is financially supported by HEAL-Link.

Notes

The authors declare no competing financial interest.

■ ACKNOWLEDGMENTS

The authors acknowledge the financial support provided by the FRESH project from the European Union's Horizon research and innovation program under Grant Agreement HORIZON-RIA-101069605.

■ REFERENCES

(1) IEA. Outlook for biogas and biomethane: Prospects for organic growth. 2025. https://www.iea.org/reports/outlook-for-biogas-and-biomethane-prospects-for-organic-growth/an-introduction-to-biogas-and-biomethane (accessed March 24, 2026).
(2) Huang, S. Y.; Huo, H. W.; Zhou, T. T.; Younas, M.; Zhao, Q. B.; Zheng, Y. M. Efficient and environmentally friendly CO_2 capture for biogas upgrading using concentrated K_2CO_3: Integration of membrane absorption and antisolvent crystallization. *Chem. Eng. J.* **2025**, *525*, No. 169892.
(3) Aghel, B.; Behaein, S.; Alobaid, F. CO_2 capture from biogas by biomass-based adsorbents: A review. *Fuel* **2022**, *328*, No. 125276.
(4) Gkotsis, P.; Peleka, E.; Zouboulis, A. Membrane-Based Technologies for Post-Combustion CO_2 Capture from Flue Gases: Recent Progress in Commonly Employed Membrane Materials. *Membranes (Basel).* **2023**, *13*, 898.
(5) Pantoleontos, G.; Koutsonikolas, D.; Asimakopoulou, A. G.; Lorentzou, S.; Karagiannakis, G. Modeling, Simulation, and Membrane Wetting Estimation in Gas−Liquid Contacting Processes Including Shell-Side Reaction: Biogas Upgrading Using DEA Solution. *Ind. Eng. Chem. Res.* **2024**, *63*, 9185−9202.
(6) IEA. *Global Energy Review 2025*; IEA, Paris, 2025. https://www.iea.org/reports/global-energy-review-2025.
(7) Aghel, B.; Behaein, S.; Wongwises, S.; Shadloo, M. S. A review of recent progress in biogas upgrading: With emphasis on carbon capture. *Biomass Bioenergy* **2022**, *160*, No. 106422.
(8) Lombardi, L.; Francini, G. Techno-economic and environmental assessment of the main biogas upgrading technologies. *Renew. Energy* **2020**, *156*, 440−458.
(9) Rodero, M. d. R.; Muñoz, R.; González-Sánchez, A.; Ruiz, H. A.; Quijano, G. Membrane materials for biogas purification and upgrading: Fundamentals, recent advances and challenges. *J. Environ. Chem. Eng.* **2024**, *12*, No. 114106.
(10) Knoope, M. M. J.; Ramírez, A.; Faaij, A. P. C. A state-of-the-art review of techno-economic models predicting the costs of CO_2 pipeline transport. *Int. J. Greenh. Gas Control* **2013**, *16*, 241−270.
(11) Budzianowski, W. M.; Wylock, C. E.; Marciniak, P. A. Power requirements of biogas upgrading by water scrubbing and biomethane compression: Comparative analysis of various plant configurations. *Energy Convers. Manag.* **2017**, *141*, 2−19.
(12) Zhang, Z.; Yan, Y.; Zhang, L.; Chen, Y.; Ran, J.; Pu, G.; Qin, C. Theoretical Study on CO_2 Absorption from Biogas by Membrane Contactors: Effect of Operating Parameters. *Ind. Eng. Chem. Res.* **2014**, *53*, 14075−14083.
(13) Baena-Moreno, F. M.; le Saché, E.; Pastor-Pérez, L.; Reina, T. R. Membrane-based technologies for biogas upgrading: a review. *Environ. Chem. Lett.* **2020**, *18*, 1649−1658.
(14) Cheng, Z.; Li, Z.; Liu, P. Amine-based CO_2 capture using hollow fiber membrane contactors in a coal-fired power plant: An absorption-desorption-combined plant-scale techno-economic analysis. *Energy* **2025**, *320*, No. 135415.
(15) Siagian, U. W. R.; Raksajati, A.; Himma, N. F.; Khoiruddin, K.; Wenten, I. G. Membrane-based carbon capture technologies: Membrane gas separation vs. membrane contactor. *J. Nat. Gas Sci. Eng.* **2019**, *67*, 172−195.
(16) Koliamitra, E.; Mitrousis, V.; Kraia, T.; Kardaras, G.; Lazaridou, N.; Grekou, T.; Fotiadis, K.; Koutsonikolas, D.; Asimakopoulou, A.; Bampaou, M.; Panopoulos, K. D. Capture, Sampling and Analysis of Biogenic CO_2 Streams for Methanol Synthesis. *Membr. 2026, Vol. 16, Page 106* **2026**, *16*, 106.
(17) Ghasem, N. Modeling and simulation of membrane-assisted separation of carbon dioxide and hydrogen from syngas. *Advances in Synthesis Gas : Methods, Technologies and Applications*; Elsevier, 2023; pp 199−218 DOI: 10.1016/B978-0-323-91879-4.00019-9.
(18) Chang, P. T.; Ng, Q. H.; Ahmad, A. L.; Oh, P. C.; Low, S. C. Development of opposing surface wettability PVDF membrane to improve CO_2 capture in membrane gas absorption. *Mater. Today Proc.* **2022**, DOI: 10.1016/j.matpr.2022.12.082.
(19) Hu, G.; Nicholas, N. J.; Smith, K. H.; Mumford, K. A.; Kentish, S. E.; Stevens, G. W. Carbon dioxide absorption into promoted potassium carbonate solutions: A review. *Int. J. Greenh. Gas Control* **2016**, *53*, 28−40.
(20) Zhang, Z. E.; Yan, Y. F.; Zhang, L.; Ju, S. X. Hollow fiber membrane contactor absorption of CO_2 from the flue gas: Review and perspective. *Glob. Nest J.* **2014**, *16*, 354−373.
(21) Gabelman, A.; Hwang, S. T. Hollow fiber membrane contactors. *J. Membr. Sci.* **1999**, *159*, 61−106.
(22) Chan, Z. P.; Li, L.; Kang, G.; Ab Manan, N.; Cao, Y.; Wang, T. Regeneration of CO_2 absorbent with membrane contactor via pressure swing. *Chem. Eng. Res. Des.* **2021**, *167*, 107−115.
(23) Kosaraju, P.; Kovvali, A. S.; Korikov, A.; Sirkar, K. K. Hollow fiber membrane contactor based CO_2 absorption-stripping using novel solvents and membranes. *Ind. Eng. Chem. Res.* **2005**, *44*, 1250−1258.
(24) Vadillo, J. M.; Gómez-Coma, L.; Garea, A.; Irabien, A. Hollow Fiber Membrane Contactors in CO_2 Desorption: A Review. *Energy Fuels* **2021**, *35*, 111−136.
(25) Sengupta, A.; Peterson, P.A. Membrane Contactor Applications in Various Industries. *Hollow Fiber Membrane Contactors*, 1st ed.; Pabby, K., Wickramasinghe, S. R., Sirkar, K. K., Sastre, A.-M., Eds.; CRC Press, 2020; pp 57−78 DOI: 10.1201/9780429398889-7.
(26) Saeed, I. M.; Alaba, P.; Mazari, S. A.; Basirun, W. J.; Lee, V. S.; Sabzoi, N. Opportunities and challenges in the development of monoethanolamine and its blends for post-combustion CO_2 capture. *Int. J. Greenh. Gas Control* **2018**, *79*, 212−233.
(27) Dubois, L.; Thomas, D. Postcombustion CO_2 capture by chemical absorption: Screening of aqueous amine(s)-based solvents. *Energy Procedia* **2013**, *37*, 1648−1657.
(28) Kim, Y. E.; Lim, J. A.; Jeong, S. K.; Yoon, Y. I.; Bae, S. T.; Nam, S. C. Comparison of carbon dioxide absorption in aqueous MEA, DEA, TEA, and AMP solutions. *Bull. Korean Chem. Soc.* **2013**, *34*, 783−787.
(29) Kim, S.; Scholes, C. A.; Heath, D. E.; Kentish, S. E. Gas-liquid membrane contactors for carbon dioxide separation: A review. *Chem. Eng. J.* **2021**, *411*, No. 128468.
(30) Cui, Z.; DeMontigny, D. Part 7: A review of CO_2 capture using hollow fiber membrane contactors. *Carbon Manag.* **2013**, *4*, 69−89.
(31) Wang, Z.; Fang, M.; Yan, S.; Yu, H.; Wei, C.-C.; Luo, Z. Optimization of Blended Amines for CO_2 Absorption in a Hollow-Fiber Membrane Contactor. *Ind. Eng. Chem. Res.* **2013**, *52*, 12170−12182.
(32) Xu, Y.; Goh, K.; Wang, R.; Bae, T.-H. A review on polymer-based membranes for gas-liquid membrane contacting processes: Current challenges and future direction. *Sep. Purif. Technol.* **2019**, *229*, No. 115791.
(33) Peeters, W.; Neerup, R.; Fosbøl, P. L. Solvent degradation & influences on amine-based carbon capture operations. *Int. J. Greenh. Gas Control* **2025**, *147*, No. 104500.

Downloaded from pubs.acs.org/iecred/article-pdf/doi/10.1021/acs.iecr.6c02581/6699023/acs.iecr.6c02581.pdf by guest on 26 August 2026

(34) Gouedard, C.; Picq, D.; Launay, F.; Carrette, P. L. Amine degradation in CO_2 capture. I. A review. *Int. J. Greenh. Gas Control* **2012**, *10*, 244−270.
(35) Zhao, F.; Cui, C.; Dong, S.; Xu, X.; Liu, H. An overview on the corrosion mechanisms and inhibition techniques for amine-based post-combustion carbon capture process. *Sep. Purif. Technol.* **2023**, *304*, No. 122091.
(36) Vega, F.; Sanna, A.; Navarrete, B.; Maroto-Valer, M. M.; Cortés, V. J. Degradation of amine-based solvents in CO_2 capture process by chemical absorption, *Greenh. Gases. Sci. Technol.* **2014**, *4*, 707−733.
(37) Sass, B.; Monzyk, B.; Ricci, S.; Gupta, A.; Hindin, B.; Gupta, N. Impact of SO_x and NO_x in Flue Gas on CO_2 Separation, Compression, and Pipeline Transmission. *Carbon Dioxide Capture for Storage in Deep Geologic Formations*; Elsevier, 2005; pp 955−981 DOI: 10.1016/B978-008044570-0/50144-6.
(38) Pantoleontos, G.; Kaldis, S. P.; Koutsonikolas, D.; Grammelis, P.; Sakellaropoulos, G. P. CO_2 Absorption in a Mini-module Membrane Contactor. *Global Warming: Engineering Solutions*; Dincer, I., Hepbasli, A., Midilli, A., Karakoc, T. H., Eds.; Springer, Boston, MA, 2010; pp 307−313 DOI: 10.1007/978-1-4419-1017-.
(39) Damartzis, T.; Asimakopoulou, A.; Koutsonikolas, D.; Skevis, G.; Georgopoulou, C.; Dimopoulos, G.; Nikolopoulos, L.; Bougiouris, K.; Richter, H.; Lubenau, U.; Economopoulos, S.; Perinu, C.; Hopkinson, D.; Panagakos, G. Solvents for Membrane-Based Post-Combustion CO_2 Capture for Potential Application in the Marine Environment. *Appl. Sci.* **2022**, *12*, 6100.
(40) Borhani, T. N. G.; Azarpour, A.; Akbari, V.; Wan Alwi, S. R.; Manan, Z. A. CO_2 capture with potassium carbonate solutions: A state-of-the-art review. *Int. J. Greenh. Gas Control* **2015**, *41*, 142−162.
(41) Niknam, M.; Zare, P.; Keshavarz, P. Experimental and modeling study of CO2 absorption by L-Proline promoted potassium carbonate using hollow fiber membrane contactor. *Int. J. Greenh. Gas Control* **2020**, *93*, No. 102877.
(42) Rouxhet, A.; Kim, S.; Leonard, G. Study of Direct Air Capture (DAC) Using a KOH/K_2CO_3 Absorbing Solution for CO_2 Capture. *SSRN Electron. J.* **2022**, DOI: 10.2139/ssrn.4273837.
(43) Comite, A.; Costa, C.; Demartini, M.; Di Felice, R.; Oliva, M. Exploring CO_2 capture from pressurized industrial gaseous effluents in membrane contactor-based pilot plant. *Int. J. Greenh. Gas Control* **2017**, *67*, 60−70.
(44) Ramezani, R.; Mazinani, S.; Di Felice, R. Characterization and kinetics of CO_2 absorption in potassium carbonate solution promoted by 2-methylpiperazine. *J. Environ. Chem. Eng.* **2018**, *6*, 3262−3272.
(45) Firman, N.; Noor, A.; Zakir, M.; Maming, M.; Fathurrahman, A. Absorption of carbon dioxide into potassium hydroxide: Preliminary study for its application into liquid scintillation counting procedure. *Egypt. J. Chem.* **2021**, *64* (9), 4907−4912.
(46) Knuutila, H.; Juliussen, O.; Svendsen, H. F. Density and N_2O solubility of sodium and potassium carbonate solutions in the temperature range 25 to 80 °C. *Chem. Eng. Sci.* **2010**, *65*, 2177−2182.
(47) Grimekis, D.; Giannoulidis, S.; Manou, K.; Panopoulos, K. D.; Karellas, S. Experimental investigation of CO_2 solubility and its absorption rate into promoted aqueous potassium carbonate solutions at elevated temperatures. *Int. J. Greenh. Gas Control* **2019**, *81*, 83−92.
(48) Vallejo Castaño, S.; Shu, Q.; Shi, M.; Blauw, R.; Loldrup Fosbøl, P.; Kuntke, P.; Tedesco, M.; Hamelers, H. V. M. Optimizing alkaline solvent regeneration through bipolar membrane electrodialysis for carbon capture. *Chem. Eng. J.* **2024**, *488*, No. 150870.
(49) Schuler, E.; Morana, M.; Ermolich, P. A.; Lüschen, K.; Greer, A. J.; Taylor, S. F. R.; Hardacre, C.; Shiju, N. R.; Gruter, G.-J. M. Formate as a key intermediate in CO_2 utilization. *Green Chem.* **2022**, *24*, 8227−8258.
(50) Abarca, J. A.; Díaz-Sainz, G.; Irabien, Á. CO_2 Electroreduction to Formate: Advancing toward Scalable Technologies. *ACS Appl. Energy Mater.* **2026**, *9*, 2041−2049.
(51) Pohorecki, R.; Moniuk, W. Kinetics of reaction between carbon dioxide and hydroxyl ions in aqueous electrolyte solutions. *Chem. Eng. Sci.* **1988**, *43*, 1677−1684.
(52) Chen, G.; Chen, G.; Cao, F.; Zhang, R.; Gao, H.; Liang, Z. Mass transfer performance and correlation for CO_2 absorption into aqueous 3-diethylaminopropylamine solution in a hollow fiber membrane contactor. *Chem. Eng. Process. - Process Intensif.* **2020**, *152*, No. 107932.
(53) Ghasem, N. Efficient CO_2 absorption through wet and falling film membrane contactors: insights from modeling and simulation. *Sci. Rep.* **2023**, *13*, 10994.
(54) Yan, Y.; Zhang, Z.; Zhang, L.; Wang, J.; Li, J.; Ju, S. Modeling of CO_2 Separation from Flue Gas by Methyldiethanolamine and 2-(1-Piperazinyl)-Ethylamine in Membrane Contactors: Effect of Gas and Liquid Parameters. *J. Energy Eng.* **2015**, *141*, No. 04014034.
(55) Gao, G.; Gao, H.; Liang, Z. Mass transfer performance and correlations for CO_2 absorption into aqueous blended PG/MEA in PTFE membrane contactor. *J. Chem. Technol. Biotechnol.* **2020**, *95*, 27−39.

Downloaded from pubs.acs.org/iecred/article-pdf/doi/10.1021/acs.iecr.6c02581/6699023/acs.iecr.6c02581.pdf by guest on 26 August 2026